New Results from the Cryogenic Dark Matter Search Experiment

D.S. Akerib,[2] J. Alvaro-Dean,[10] M.S. Armel,[10] M.J. Attisha,[1] L. Baudis,[9] D.A. Bauer,[11] A.I. Bolozdynya,[2]
P.L. Brink,[9] R. Bunker,[11] B. Cabrera,[9] D.O. Caldwell,[11] J.P. Castle,[9] C.L. Chang,[9] R.M. Clarke,[9] M.B. Crisler,[3]
P. Cushman,[8] A.K. Davies,[9] R. Dixon,[3] D.D. Driscoll,[2] L. Duong,[8] J. Emes,[4] R. Ferril,[11] R.J. Gaitskell,[1]
S.R. Golwala,[10] M. Haldeman,[3] J. Hellmig,[10] M. Hennessey,[9] D. Holmgren,[3] M.E. Huber,[12] S. Kamat,[2]
M. Kurylowicz,[9] A. Lu,[10] R. Mahapatra,[11] V. Mandic,[10] J.M. Martinis,[5] P. Meunier,[10] N. Mirabolfathi,[10]
S.W. Nam,[9] H. Nelson,[11] R. Nelson,[11] R.W. Ogburn,[9] J. Perales,[9] T.A. Perera,[2] M.C. Perillo Isaac,[10] W. Rau,[10]
A. Reisetter,[8] R.R. Ross,[4, 10] T. Saab,[9] B. Sadoulet,[4, 10] J. Sander,[11] C. Savage,[11] R.W. Schnee,[2] D.N. Seitz,[10]
T.A. Shutt,[6] G. Smith,[10] A.L. Spadafora,[10] J-P.F. Thompson,[1] A. Tomada,[9] G. Wang,[2] S. Yellin,[11] and B.A. Young[7]

(CDMS Collaboration)

[1]*Department of Physics, Brown University, Providence, RI 02912, USA*
[2]*Department of Physics, Case Western Reserve University, Cleveland, OH 44106, USA*
[3]*Fermi National Accelerator Laboratory, Batavia, IL 60510, USA*
[4]*Lawrence Berkeley National Laboratory, Berkeley, CA 94720, USA*
[5]*National Institute of Standards and Technology, Boulder, CO 80303, USA*
[6]*Department of Physics, Princeton University, Princeton, NJ 08544, USA*
[7]*Department of Physics, Santa Clara University, Santa Clara, CA 95053, USA*
[8]*School of Physics & Astronomy, University of Minnesota, Minneapolis, MN 55455, USA*
[9]*Department of Physics, Stanford University, Stanford, CA 94305, USA*
[10]*Department of Physics, University of California, Berkeley, CA 94720, USA*
[11]*Department of Physics, University of California, Santa Barbara, CA 93106, USA*
[12]*Department of Physics, University of Colorado at Denver, Denver, CO 80217, USA*
(Dated: February 7, 2008)

Using improved Ge and Si detectors, better neutron shielding, and increased counting time, the Cryogenic Dark Matter Search (CDMS) experiment has obtained stricter limits on the cross section of weakly interacting massive particles (WIMPs) elastically scattering from nuclei. Increased discrimination against electromagnetic backgrounds and reduction of the neutron flux confirm WIMP-candidate events previously detected by CDMS were consistent with neutrons and give limits on spin-independent WIMP interactions which are $> 2\times$ lower than previous CDMS results for high WIMP mass, and which exclude new parameter space for WIMPs with mass between 8–20 GeV c^{-2}.

PACS numbers: 26.65.+t, 95.75.Wx, 14.60.St

This Letter reports new exclusion limits from the Cryogenic Dark Matter Search (CDMS) experiment on the wide class of nonluminous, nonbaryonic, weakly interacting massive particles (WIMPs) [1, 2] which could constitute most of the matter in the universe [3]. A natural WIMP candidate is provided by supersymmetry in the form of the stable lightest superpartner, usually taken to be a neutralino of typical mass ~ 100 GeV/c^2 [2, 4]. Since the WIMPs are expected to be in a roughly isothermal halo within which the visible portion of our galaxy resides, the energy given to a Ge or Si detector nucleus scattered elastically by a WIMP would be only a few to tens of keV [5].

Because of this low recoil energy and very low event rate (< 1 event per day per kg of detector mass), it is essential to suppress backgrounds drastically. The CDMS detectors discriminate nuclear recoils (such as would be produced by WIMPs) from electron recoils by measuring both ionization and phonon energy, greatly reducing the otherwise dominant electromagnetic background. The ionization is much less for nuclear than for electron recoils, while the phonon signal enables a determination

of the recoil energy. The main remaining background is from neutrons, which produce WIMP-like recoils, and hence must be distinguished by other means. Two are employed: 1) while Ge and Si have similar scattering rates per nucleon for neutrons, Ge is 5–7 times more efficient than Si for coherently scattering WIMPs; 2) a single WIMP will not scatter in more than one detector, while a neutron frequently will.

While brief reviews of all parts of the experiment are provided below, most details have been published [6], and therefore the emphasis here will be on the differences from previous work. The previously published results are from three 165 g Ge BLIP (Berkeley Large Ionization-and-Phonon-mediated) and one 100 g Si ZIP (Z-sensitive Ionization and Phonon-mediated) detectors. The latter, employed as one measure of background neutrons, was not used simultaneously with the Ge BLIPs, but rather in a separate run. BLIP detectors determine phonon production from the detector's calorimetric temperature change, whereas ZIP detectors [7] collect athermal phonons to provide both phonon production and position information. Position information can be obtained

from pulse arrival times and relative signal sizes in multiple sensors. Pulse rise time gives further discrimination against surface events which could otherwise be misidentified as nuclear recoils. The new experiment used four 250 g Ge and two 100 g Si ZIP detectors simultaneously, improving measurement of neutron backgrounds.

Since new detector technologies were used, both CDMS experiments operated at a convenient shallow site. The experiments had an overburden of 16 meters water equivalent, sufficient to stop the hadronic cosmic ray component and reduce the muon flux by a factor of 5. The apparatus from outside to inside included a plastic-scintillator veto to reject muon-coincident particles by a factor of $> 10^3$, a 15-cm-thick lead shield to reduce background photon flux by a factor of 10^3, 25 cm of polyethylene, a 20 mK volume provided by a custom, radiopure side extension to an Oxford 400S dilution refrigerator [8], and 1 cm of ancient Pb. In the new experiment 11 kg of polyethylene added inside the ancient Pb reduced the neutrons by a factor of 2.3, not only making this a better measurement, but also confirming the neutron level given in the previously published experiment.

Because detector discrimination reduced electromagnetic backgrounds, the limiting background was from relatively rare, high-energy neutrons produced outside the veto. The neutrons may "punch through" the shielding and yield secondary neutrons whose scatters in the detectors can mimic the WIMP signal [6]. As in the previous experiment, the propagation of these neutrons was simulated accurately, as confirmed by comparison with veto-coincident and calibration-source neutrons. There is excellent agreement of the simulated and observed recoil-energy spectra. No experimental results depend on any *a priori* knowledge of the absolute value of the neutron background.

The utility of the simulations lies in predicting the relative rates of neutron events in the Ge and Si detectors, and the relative number of neutron scatters in a single detector to that in multiple detectors. These predicted ratios and the observed numbers of multiple-detector and Si neutrons determine the single-scatter neutron background in the Ge detectors. A check on the consistency of the null hypothesis that all candidate events in the previous and present experiments are neutrons is provided by comparing the numbers of observed and predicted events in the two experiments simultaneously. Assuming all events are due to neutrons and taking into account the different polyethylene shielding, the numbers of Ge and Si singles and multiples observed in the two experiments all agree with the same incident neutron flux.

The new 1-cm-thick, 7.62-cm-diameter detectors were stacked 3.5 mm apart with no intervening material. The ionization electrodes deposited on the bottom surface of each detector were divided into an annular outer part shielding the disk-shaped inner part from any low-energy electrons emitted from surrounding surfaces. The disk part constituted 85% of the physical volume in the new experiment in contrast to $\sim 56\%$ previously. The disk areas at only the top and bottom of the stack were exposed to external materials. A Si detector, known to have had some exposure to ^{14}C contamination during a previous run, was placed on the bottom and was used for multiple scatters but not for singles data. The Ge detector requiring a 20-keV analysis threshold was put at the top. All other detectors (from top to bottom: Ge, Ge, Si, Ge) had analysis thresholds of 5 keV, compared to the 10-keV thresholds used in the previous experiment. The analysis threshold was well above the phonon-trigger threshold of ~ 2 keV and the $\sim$1.5 keV (for electron recoils) search threshold for ionization from the disk region.

Thresholds were determined by how well the detector's ionization yield, Y, the ratio of ionization production to recoil energy (using also the phonon signal), separates electron from nuclear recoils. Photons cause most bulk electron recoils, while low-energy electrons can cause low-Y electron recoils in a thin surface layer, possibly resulting in confusion with nuclear recoils. In this experiment ZIP detectors provided additional rejection of such surface events by pulse rise time information, which is sensitive to the depth of the interaction. Neutron and photon sources were used to determine efficiencies for discrimination between nuclear recoils and bulk and surface electron events. These calibration runs established the acceptable nuclear—and hence WIMP—recoil band. Figure 1 illustrates the particle discrimination, which can be characterized by a photon rejection $> 99.98\%$ (5–100 keV) and an electron rejection $> 99\%$ above 10 keV for the four central detectors, far exceeding those (99.9% and 95%, respectively) of the previous experiment.

The data set of the present experiment was taken with a 3 V bias voltage across the detector ionization electrodes used to collect the electrons and holes. A data set to be reported later employed a 6 V bias. The larger voltage improves the ionization yield of surface electron events but results in worse rise-time-based particle discrimination. At 3 V bias, 93 days of low-background data were taken from December 2001 to April 2002, resulting in 65.8 live days and 4.6×10^6 events. After cuts this became 28.3 kg-d of data, substantially more than the 15.8 kg-d of the previous experiment. Three calibrations with ^{60}Co photon sources and two with ^{252}Cf neutron sources were performed at various times during the run.

The position information available from the ZIP detectors was used to make small corrections for variations of the phonon signal with event location. The corrections for this position dependence, improving the phonon energy resolution and the surface electron rejection, were obtained from the photon calibration.

Most cut parameters were set based on calibration data, and all cuts except the threshold-energy cut for the top detector were set before examining the final 90% of the low-background data. The cut for data quality had
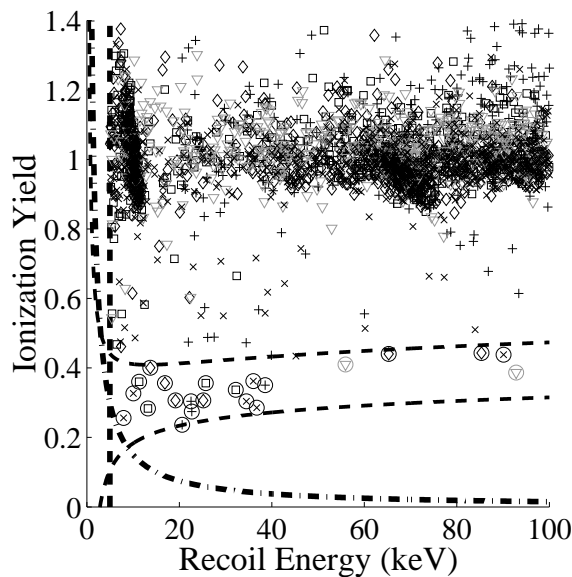
FIG. 1: Ionization yield (Y) vs. recoil energy for veto-anticoincident single scatters in the 4 Ge (black ×, diamond, square, and +) and 1 inner Si (grey triangle) detectors above the 5 keV analysis threshold (dashed vertical line). Twenty events (circled) lie within the mean nominal 95% nuclear-recoil acceptance region (dashed curves), above the ionization threshold (dot-dashed curve). Most of the events with $0.5 < Y < 0.8$ are in the top Ge detector (×), whose top face is unshielded, or in the bottom Ge detector (+), whose bottom disk region faces the contaminated Si detector.

> 99.99% efficiency. Having at least 80% of the ionization energy in the disk part of the detector and having phonon rise time $> 12 \mu$s for Ge and $> 6 \mu$s for Si gave an energy-dependent efficiency for nuclear-recoil events varying from 10–15% at 5 keV to 40–45% at 20 keV to 50-60% at higher energies. Requiring $> 40 \mu$s after the most recent muon veto gave an $\sim 80\%$ efficiency for a typical 5.2 kHz veto rate. Selecting a nuclear-recoil band in Y within $\pm 2 \sigma$ of the band mean gave 95% efficiency for nuclear-recoil events.

Nuclear-recoil, single-scattering candidates satisfied all the above cuts and had energy above both the ionization and phonon thresholds in one detector, but no phonon trigger in any other detector within 50 μs of the event trigger. Nuclear-recoil, multiple-scattering candidates required passing data-quality and veto-anticoincident cuts, all triggering detectors having between 5–100 keV of recoil energy (and at least 80% of their ionization energy in their disk region), at least two of the detectors passing the nuclear-recoil cut, and at least one of the detectors passing the rise-time cut.

A histogram of the 20 Ge single-scatter nuclear-recoil candidates as a function of energy is shown in Fig. 2, along with the expected neutron spectrum. This simulated neutron spectrum agrees well with the data, as is verified by a Kolmogorov-Smirnov test. These 20 can-
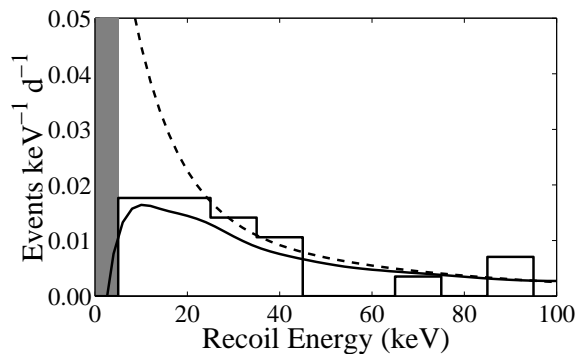

FIG. 2: Histogram in 10-keV bins of the 20 veto-anticoincident, single-scatter nuclear-recoil candidates observed in the 4 Ge detectors of total mass 1 kg. The dashed curve is the shape of the expected recoil-energy spectrum due to incident neutrons, while the solid curve also takes into account the detection efficiency and is normalized to 20 events.

didates could include some surface-electron events. The expected number of such events in the nuclear-recoil band is 1.2 ± 0.3 in the Ge detectors and 0.8 ± 0.6 in the Si detector. The expected contamination was found from maximum likelihood fits to the rise time and yield (Y) distribution of the $\sim 1\%$ of photon calibration events occurring near the surface. The fits were normalized to the observed number of background surface events outside the signal region.

The 90% CL excluded region for the WIMP mass M and the spin-independent WIMP-nucleon elastic-scattering cross-section σ is derived using a likelihood ratio approach and conservative parameter values as described in [6]. This method accounts for those observed Ge single scatters that are due to the unvetoed neutron flux, as constrained by the observed 2 triple scatters and 1 non-nearest-neighbor double scatter (shown in Fig. 3), along with 2 single-scatter nuclear-recoil candidates in the Si detector. Nearest-neighbor double scattering events were not used to determine the number of neutrons in the Ge single-scatter sample because correction for false events due to double scattering of surface electrons is too uncertain at this time.

Figure 4 displays the resulting upper limits on the spin-independent WIMP-nucleon elastic-scattering cross-section. Because the neutron simulation predicts 5.3 Ge singles per multiple-detector neutron, all the nuclear recoils may be neutron scatters and $\sigma = 0$ is not excluded. The dip in the limit curve is due to the fact that low-mass WIMPs could not cause the several detected events between $\sim$30–40 keV. Figure 4 also shows the upper limits calculated ignoring all information about the neutron background, using Yellin's "Optimum Interval" method [9]. The limit is essentially set by a region of the energy spectrum with few events compared to the number expected from the WIMP energy spectrum. Because of the weak statistical power gained by estimat-
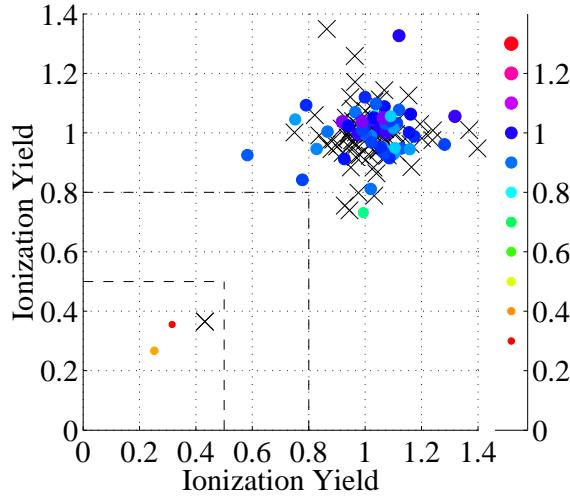
FIG. 3: Scatter plot of ionization yields for veto-anticoincident triple scatters (filled circles) and non-nearest-neighbor double scatters (×'s) with all scatters between 5 and 100 keV and within the fiducial volume. For triple scatters, the size and color of the circle indicates the ionization yield in the third detector. Note both neutron triple-scatter candidates show low yield in all three detectors, while no other triple scatters have low yield in any detector. As expected for such events, there is clearly negligible contamination from surface events.

ing the neutron background based on the small number of multiple-scatter and Si events, the sensitivity without subtraction of the neutron background is nearly as good as the sensitivity including subtraction of the neutron background. These limits exclude new parameter space for WIMPs with $8 < M < 20$ GeV c^{-2}. Furthermore, a simultaneous goodness-of-fit test (as described in [6]), indicates the model-independent annual-modulation signal of DAMA (as shown in Fig. 2 of [11]) and these CDMS data are incompatible at 99.98% CL, if the WIMP interactions and halo are standard.

[1] B.W. Lee and S. Weinberg, Phys. Rev. Lett. **39**, 165 (1977).

[2] G. Jungman, M. Kamionkowski, and K. Griest, Phys. Rep. **267**, 195 (1996).

[3] L. Bergstrom, Rep. Prog. Phys. **63**, 793 (2000); M. Srednicki, Eur. J. Phys. C. **15**, 143 (2000); P.J.E. Peebles, Principles of Physical Cosmology (Princeton University Press, Princeton, NJ, 1993).
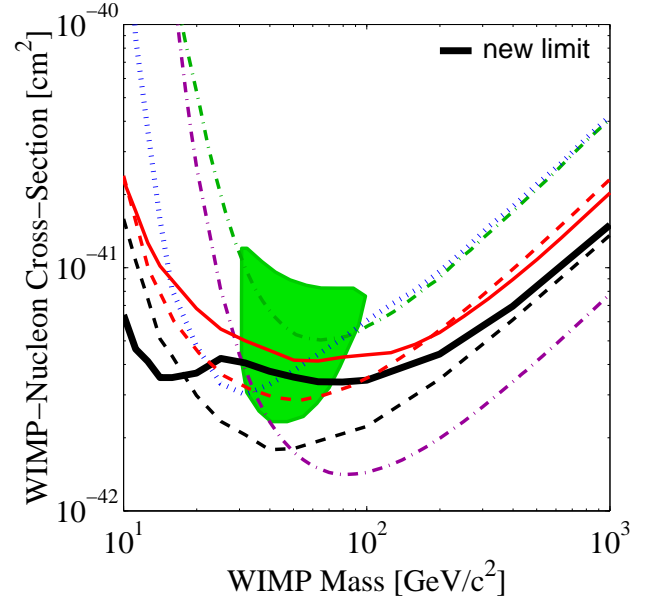

FIG. 4: Spin-independent σ vs. M. The regions above the curves are excluded at 90% CL. Solid, thick black curve: limit from this analysis including statistical subtraction of the neutron background. Solid red curve: limit from this analysis without statistical subtraction of the neutron background. Dashed curves: CDMS expected sensitivity (median simulated limit) given the expected neutron background (as normalized based on this and previous work) of 3.3 multiple-scatters, 18 single scatters in Ge, and an expected background in Si of 0.8 electrons and 3.6 neutrons, with (black) or without (red) neutron subtraction. Blue dotted curve: previous CDMS upper limit [6]. Green dot-dashed curve: DAMA limit using pulse-shape analysis [10]. The DAMA 3σ allowed region not including the DAMA limit [11] is shown as a shaded region. Above 30 GeV c^{-2}, the EDELWEISS [12] (purple dot-dashed curve) experiment provides more sensitive limits. All curves are normalized following [5], using the Helm spin-independent form-factor, A^2 scaling, WIMP characteristic velocity $v_0 = 220$ km s^{-1}, mean Earth velocity $v_E = 232$ km s^{-1}, and $\rho = 0.3$ GeV c^{-2} cm^{-3}.

[4] J. Ellis, T. Falk, K.A. Olive, and M. Schmitt, Phys. Lett. **B413**, 355 (1997); J. Edsjo and P. Gondolo, Phys. Rev. D **56**, 1879 (1997); A. Bottino, F. Donato, N. Fornengo, and S. Scopel, Phys. Rev. D **63**, 125003 (2001).

[5] J.D. Lewin and P.F. Smith, Astropart. Phys. **6**, 87 (1996).

[6] D. Abrams et al., Phys. Rev. D **66**, 122003 (2002).

[7] K.D. Irwin et al., Rev. Sci. Instr. **66**, 5322 (1995); R.M. Clarke et al., in *Proceedings of the Second International Workshop on the Identification of Dark Matter*, edited by N.J.C. Spooner and V. Kudryavtsev (World Scientific, Singapore, 1999), pp. 353-358; T. Saab et al., *AIP Proc.* **605**, 497 (2002).

[8] J.D. Taylor et al., Adv. Cryo. Eng. **41**, 1971 (1996); A. Da Silva et al., Nucl. Instr. Meth. A **354**, 553 (1995).

[9] S. Yellin, Phys. Rev. D **66**, 032005 (2002).

[10] R. Bernabei et al., Phys. Lett. **B389**, 757 (1996).

[11] R. Bernabei et al., Phys. Lett. **B480**, 23 (2000).

[12] A. Benoit et al., Phys. Lett. **B545**, 43 (2002).